Prephase-Based Equivalent Amplitude Tailoring for Low Sidelobe Levels of 1-Bit Phase-Only Control Metasurface under Plane Wave Incidence

Jiexi Yin [1], Qi Wu [1], Haiming Wang [2], and Zhining Chen [1]

[1]Affiliation not available
[2]Southeast University

October 30, 2023

Abstract

A prephase synthesis method is proposed for sidelobe level (SLL) suppression of a 1-bit phase-only control metasurface under plane wave incidence. The array factor of the metasurface with N×N unit cells shows that controlling the number of prephases with varying values over the reflective surface realizes equivalent amplitude tailoring. Different from optimizing the prephase distribution, selection of the numbers of 0 and $\pi/2$ prephases in specific N regions is used to suppress the SLLs. Therefore, the parameters in the optimization can be dramatically reduced from N^2 to N. The prephase distribution is then designed based on the optimized number of prephases and a symmetric matrix for SLL suppression in the whole space. The SLLs are further suppressed by optimizing some of the unit cell states based on similar equivalent amplitude tailoring. Simulation and measurement of a set of 1-bit reflective metasurfaces with 20×20 unit cells verify that the phase-only control metasurface realizes SLL suppression to -13 dB for multiple beam directions from -30 to 30 degrees with a 10-degree step under normal plane wave incidence.

Prephase-Based Equivalent Amplitude Tailoring for Low Sidelobe Levels of 1-Bit Phase-Only Control Metasurface under Plane Wave Incidence

Jiexi Yin, *Member, IEEE*, Qi Wu, *Member, IEEE*, Haiming Wang, *Member, IEEE*, and Zhi Ning Chen, *Fellow, IEEE*

***Abstract*—A prephase synthesis method is proposed for sidelobe level (SLL) suppression of a 1-bit phase-only control metasurface under plane wave incidence. The array factor of the metasurface with $N \times N$ unit cells shows that controlling the number of prephases with varying values over the reflective surface realizes equivalent amplitude tailoring. Different from optimizing the prephase distribution, selection of the numbers of 0 and $\pi/2$ prephases in specific N regions is used to suppress the SLLs. Therefore, the parameters in the optimization can be dramatically reduced from N^2 to N. The prephase distribution is then designed based on the optimized number of prephases and a symmetric matrix for SLL suppression in the whole space. The SLLs are further suppressed by optimizing some of the unit cell states based on similar equivalent amplitude tailoring. Simulation and measurement of a set of 1-bit reflective metasurfaces with 20×20 unit cells verify that the phase-only control metasurface realizes SLL suppression to -13 dB for multiple beam directions from -30 to 30 degrees with a 10-degree step under normal plane wave incidence.**

***Index Terms*—Single-beam, 1-bit, plane waves, reflective metasurface, sidelobe level (SLL), phase control.**

I. Introduction

BEAMFORMING and beam scanning are essential requirements for 5G millimeter wave (mmWave) communications [1], [2]. Reflective metasurfaces have a beamforming capability by controlling the phases of the unit cells [3], [4]. Reconfigurable reflective metasurfaces can be designed using discrete phase compensations, such as 1-bit phase compensation, to achieve beam scanning performance [5], [6].

For mmWave communications, systems focus electromagnetic wave radiation in desired directions and suppress radiation in other directions [7]. Therefore, a pencil beam with low sidelobe levels (SLLs) is preferred. On the one hand, pencil beams with high gain can be realized using reflective metasurfaces excited by spherical waves. The spherical waves introduce an intrinsic pseudorandom distribution of the phase quantization error to form a single beam [8], [9]. Furthermore, the spherical wave incidence also brings a nonuniform amplitude distribution on the reflective surfaces, which helps suppress SLLs. For example, a 1-bit reflective metasurface based on a linear polarizer achieves a fixed beam with an SLL of -14 dB [10], and a 1-bit reconfigurable reflective metasurface achieves beam scanning with an SLL of -10 dB [11]. One-bit phase-controlled reflective metasurfaces under spherical wave incidence can usually realize single-beam patterns with SLLs from -20 to -10 dB [10]–[15].

On the other hand, reflective surfaces also work under plane wave incidence [16], such as when controlling the propagation paths of electromagnetic (EM) waves for mmWave indoor communications [17]. Unlike spherical wave incidence, plane wave incidence brings a uniform amplitude distribution on the reflective surface. Moreover, the initial phases on the reflective surfaces are the same without a gradient for normal plane wave incidence. The same initial phases usually cause symmetric beams for single-beam forming when using 1-bit phase compensation. Even if oblique wave incidence brings a gradient initial phase distribution, the SLLs are usually very high because of quasiperiodic phase quantization errors [9]. Therefore, there are more challenges in 1-bit single-beam design and SLL suppression under plane wave incidence than under spherical wave incidence. Although 1-bit reflective metasurfaces with randomized phase quantization errors can effectively suppress symmetric beams [18], the worst SLL is larger than -8 dB for beam scanning [19] because of the uniform amplitude distribution on the reflective surfaces brought by the plane waves and the fixed pseudorandom uniform prephase distribution that cannot ensure SLL suppression in all beam directions.

An SLL suppression method for 1-bit single-beam reflective metasurfaces under normal plane wave incidence is proposed in this work. First, a theoretical analysis proves that control of the prephase distribution can be to some degree equivalent to

Manuscript received Dec. 5, 2021; revised , ; accepted , . Date of publication , ; date of current , . This work was supported in part by the National Key R&D Program of China under Grant 2020YFB1804901, the National Natural Science Foundation of China under Grants 61671145 and 61960206006, the Key R&D Program of Jiangsu Province of China under Grant BE2018121, and the Ministry of Education of Singapore under Grant R-263-000-E86-112. *(Corresponding author: Haiming Wang.)*

J. X. Yin was with the State Key Laboratory of Millimeter Waves and the School of Information Science and Engineering, Southeast University, Nanjing 210096, China, and is now with the Department of Electrical and Computer Engineering, National University of Singapore, Singapore 117583 (e-mail: jiexiyin@ieee.org).

Q. Wu and H. M. Wang are with the State Key Laboratory of Millimeter Waves and the School of Information Science and Engineering, Southeast University, Nanjing 210096, China, and with the Purple Mountain Laboratories, Nanjing 211111, China (e-mail: qiwu@seu.edu.cn; hmwang@seu.edu.cn).

Z. N. Chen is with the Department of Electrical and Computer Engineering, National University of Singapore, Singapore 117583 (e-mail: eleczn@nus.edu.sg).

Color versions of one or more of the figures in this paper are available online at http://ieeexplore.ieee.org.

Digital Object Identifier

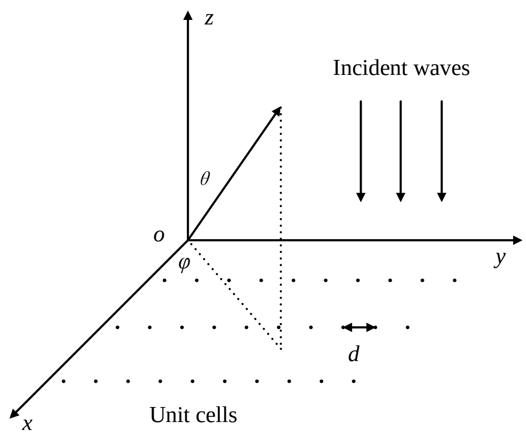

Fig. 1. Geometry of the 1-bit array under normal plane wave incidence.

amplitude control. By controlling the number of two different prephases rather than optimizing the prephase distribution, the optimization can be reduced from N^2 prephase parameters to N. Next, the phase design and optimization of the metasurface are described in detail, both for the prephase distribution and 1-bit states of unit cells. Finally, a set of 1-bit single-beam reflective metasurfaces with the same prephase distribution for different beam directions to suppress the SLLs are designed, fabricated, and measured.

II. Theoretical Analysis of Prephase Design Equivalent to Amplitude Tailoring

Assume that the 1-bit reflective metasurface has $N \times N$ unit cells with uniform interelement spacing d, as shown in Fig. 1. The unit cells are simplified as point sources. That is, only the array factor is considered in the theoretical study. The prephase is introduced to each unit cell for single beamforming [19]. Under normal plane wave incidence, all unit cells have a uniform amplitude and the same initial phase, and the array factor $\mathrm{AF}(\theta, \varphi)$ can be derived as

$$\mathrm{AF}(\theta, \varphi) = \sum_{s=1}^{N} \sum_{k=1}^{N} e^{j\Phi_{s,k}(\theta,\varphi)}, \tag{1}$$

where θ and φ represent the elevation angle and the azimuth angle, respectively, and $s, k = 1, 2, ..., N$. The total phase of the unit cell $\Phi_{s,k}(\theta, \varphi)$ in the s-th row and k-th column is the sum of the 1-bit phase compensation $\phi_{(s,k)}$, the prephase $\psi_{(s,k)}$, and the progressive phase $\zeta_{(s,k)}(\theta, \varphi)$, that is,

$$\Phi_{s,k}(\theta, \varphi) = \phi_{s,k} + \psi_{s,k} + \zeta_{s,k}(\theta, \varphi), \tag{2}$$

with

$$\zeta_{s,k}(\theta, \varphi) = \frac{2\pi d}{\lambda} \sin\theta((s-1)\cos\varphi + (k-1)\sin\varphi), \tag{3}$$

and λ being the wavelength of the carrier frequency in vacuum.

To maximize energy in the desired beam direction, the ideal phase compensation $\phi^{'}(s, k)$ for each unit cell is usually calculated:

$$\begin{aligned} \phi^{'}_{s,k} = &-\frac{2\pi}{\lambda}\sin\theta_i((s-1)\cos\varphi_i + (k-1)\sin\varphi_i) \\ &-\psi_{s,k} + \phi_i, \end{aligned} \tag{4}$$

where $(\theta_i,\ \varphi_i)$ is the designed beam direction (i = 0,1,2...) and constant ϕ_i is the reference phase [8]. Without loss of generality, the states of the unit cell can be determined:

$$\phi_{s,k} = \begin{cases} 0 & \bmod\ (\phi^{'}_{s,k}, 2\pi) \in [-\frac{\pi}{2}, \frac{\pi}{2}), \quad \text{State}\, 0, \\ \pi & \bmod\ (\phi^{'}_{s,k}, 2\pi) \in [\frac{\pi}{2}, \frac{3\pi}{2}), \quad \text{State}\, 1. \end{cases} \tag{5}$$

For normally incident plane waves, once the prephase distribution and designed beam direction θ_i, φ_i are given, the states of the unit cells are determined by (4) and (5). For different i, the unit cell states usually change, but with the same prephase. The SLL can be obtained from $\mathrm{AF}(\theta, \varphi)$.

$$g(\psi_{s,k}, \phi_{s,k}) = \min(af_1, \mathrm{AF}(\theta_i, \varphi_i)) - af_2, \tag{6}$$

where $\{af_1,\ af_2,\ af_3 ... af_n\}$ are a set of local maxima of $\mathrm{AF}(\theta, \varphi)$, with $af_1 \geq af_2 \geq af_3 \geq ... \geq af_{n-1} \geq af_n$.

The SLL depends on the prephase distribution $\psi_{s,k}$ and 1-bit phase compensation $\phi_{s,k}$. Because $\phi_{s,k}$ can be calculated when $\psi_{s,k}$ and the beam direction $(\theta_i,\ \varphi_i)$ are given, the optimization of $g(\psi_{s,k}, \phi_{s,k})$ can be presented as

$$\arg \max_{\psi_{s,k} \in [0, 2\pi)} \sum_i g(\psi_{s,k}). \tag{7}$$

The SLLs are determined by prephase distribution $\psi_{s,k}$ with N^2 parameters (assuming that the reference phase is optimal).

In the xoz plane, $\varphi = 0$, so (3) can be simplified as

$$\zeta_{s,k}(\theta, 0) = (s-1)\frac{2\pi d}{\lambda} \sin\theta, \tag{8}$$

and $\zeta_{s,k}$ is the same for the same column (k) because of the orthogonality of the x-direction and y-direction. Furthermore, according to (4), the states of unit cells for the same prephase and column are the same if the designed beam is in the xoz plane.

As discussed in reference [19], at least two kinds of prephases should be introduced for single-beam forming, and a $\pi/2$ phase difference can achieve a noneven function of $\mathrm{AF}(\theta, \varphi)$ and break the symmetry. Thus, 0 and $\pi/2$ are chosen as the two kinds of prephases in this study. If there are x_k ($x_k \in \{0, 1, 2, ..., N\}$) prephases of 0 and $(N - x_k)$ prephases of $\pi/2$ in the k-th column, then $\mathrm{AF}(\theta, 0)$ can be derived as

$$\begin{aligned} \mathrm{AF}(\theta, 0) &= \sum_{k=1}^{N} (x_k e^{j(\psi_{k_1} + 0 + (k-1)\frac{2\pi d}{\lambda}\sin\theta)} \\ &\quad + (N - x_k) e^{j(\psi_{k_2} + \pi/2 + (k-1)\frac{2\pi d}{\lambda}\sin\theta)}) \\ &= \sum_{k=1}^{N} \mathrm{AF_k}(\theta, 0). \end{aligned} \tag{9}$$

ψ_{k_1} and $\psi_{k_2} \in (0,\ \pi)$ represent the 1-bit phase compensation of the unit cells. The SLLs in the xoz plane only depend on parameters x_k, and the optimization of (7) can be simplified as

$$\arg \max_{x_k \in \{0,1,2...,N\}} \sum_i g_{xoz}(x_k), \tag{10}$$

where $g_{xoz}(x_k)$ presents the SLL in the scanning plane (xoz plane) with φ_i = 0 and φ = 0.

Let $|\mathrm{AF_k}(\theta,0)|$ represents the amplitude contribution of the k-th column and

$$|\mathrm{AF}_k(\theta,0)| = ({x_k}^2 + (N-x_k)^2 + 2x_n(N-x_k)\cos(\phi_{k_1}-\phi_{k_2}-\pi/2))^{\frac{1}{2}}. \tag{11}$$

Considering 1-bit phase compensation, $(\phi_{k_1}-\phi_{k_2})$ can be chosen only among $-\pi$, 0, and π. Therefore, (11) can be further simplified into

$$|\mathrm{AF}_k(\theta,0)| = ({x_k}^2 + (N-x_k)^2)^{\frac{1}{2}}. \tag{12}$$

$|\mathrm{AF}_k(\theta,0)|$ can range from $\sqrt{2}N/2$ to N with different x_k. Therefore, if we only consider the 2D patterns in the xoz plane, the equivalent amplitudes $|\mathrm{AF}_k(\theta,0)|$ can be controlled using different numbers of prephases of 0 and $\pi/2$. For example, when all prephases in the k-th column are the same, $|\mathrm{AF}_k(\theta,0)|$ will obtain the maximum value; when the number of 0 prephases is the same as the number of $\pi/2$ prephases, $|\mathrm{AF}_k(\theta,0)|$ will obtain the minimum value. The SLLs can be improved by controlling $|\mathrm{AF}_k(\theta,0)|$.

However, because of 1-bit phase compensation, in the design of the prephase distribution, suppression of symmetric beams should also be considered. The equivalent phases of $\mathrm{AF}_k(\theta,0)$ are usually different for different k. Some classical amplitude distributions, such as the Chebyshev distribution, usually default to the unit cell providing perfect phases and amplitudes. Therefore, these classical amplitude distributions may not be suitable for this design. The phase design and SLL suppression will be discussed in detail in the next section.

III. SLL Optimization for a Planar Array

In the phase-only control metasurface design, the number of unit cells and the interelement spacing also influence the SLLs. For comparison with the results in [19], the same setup with $N = 20$ and $d = \lambda/2$ is discussed as an example. The designed scanning range is from -30 to 30 degrees with a 10 degree step, and all unit cells have a uniform amplitude.

The workflow of SLL suppression is illustrated in Fig. 2. For the desired beam scanning range, a fixed prephase distribution should be designed for different beam directions θ_i. Based on the theory in Section II and inspired by the concept of dimensionality reduction (DR) [20], [21], the optimization of $\psi_{s,k}$ is transformed into optimization of x_k, and a 2D planar array is converted into a 1D linear array in the optimization. The method considers the equivalent amplitude and retains the pattern messages after DR. Then, a symmetric matrix is utilized to recover the planar array from the linear array. Next, the states of 1-bit unit cells for desired beam directions are designed considering the gain and SLL. Finally, SLL suppression is achieved by controlling the phase distributions (prephases and states) on the reflective metasurface. The detailed principles and methods are presented as follows.

A. Prephase Optimization for a Planar Array

To obtain the maximal radar cross-section (RCS) in the desired directions, the states of the unit cells can be calculated using (4) and (5) when the reference phase and the beam direction are given. For different directions, the fixed prephase distribution dramatically influences the symmetric beams and SLLs. Although a pseudorandom uniformly distributed prephase can effectively suppress symmetric beams for beam scanning, it cannot ensure SLL suppression for each beam direction. For example, the worst SLL of a prephased planar array is -7.7 dB for scanning from -30 to 30 degrees with a 10 degree step ($N = 20$, $d = \lambda/2$), as shown in Fig. 3(a). Although reference phases can be introduced in every beam direction to improve the patterns, the worst SLL is still larger than -8.0 dB, as shown in Fig. 3(b).

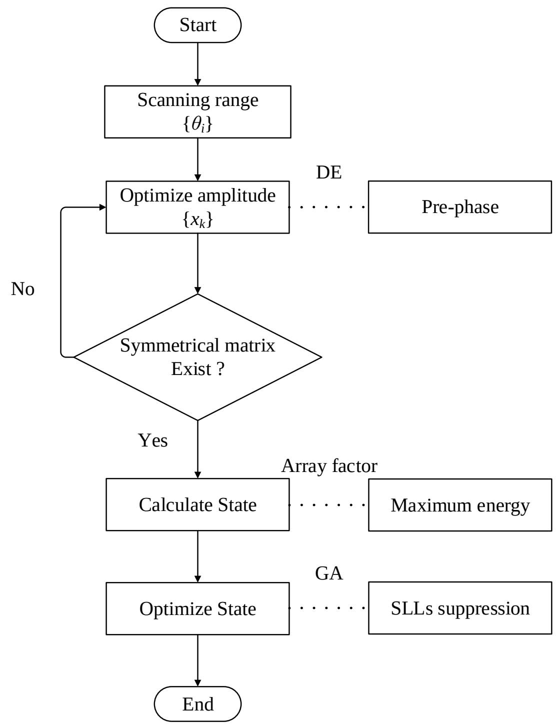

Fig. 2. Flow diagram of the SLL optimization for a planar array.

For a reflective metasurface with $N \times N$ unit cells, N^2 prephases can be optimized, which may bring considerable complexity. According to the analysis of Section II, for the patterns in the beam scanning plane, control of the prephase distribution can provide equivalent amplitude tailoring, and optimization of the prephase distribution can be transformed in to optimization of the numbers of 0 and $\pi/2$ prephases in each column. Therefore, only N parameters are required for x_k optimization, rather than the N^2 prephases for $\psi_{s,k}$ optimization.

If the designed beams are in the xoz plane, then equivalent amplitude control can be realized when using different numbers of 0 and $\pi/2$ prephases in each column. The patterns depend on the equivalent modulus and the equivalent phase of $\mathrm{AF}_k(\theta,0)$. Therefore, we first optimize x_k to improve the patterns in the scanning plane, i.e., the xoz plane. For the k-th column, there are x_k elements with 0 prephase and (N- x_k) elements with $\pi/2$ prephase (n = 1,2,3,...,N). Thus, only N parameters need to be optimized, and the prephase design can be simplified. According to (9), the SLLs can be obtained and optimized based on different combinations of x_k. Using the

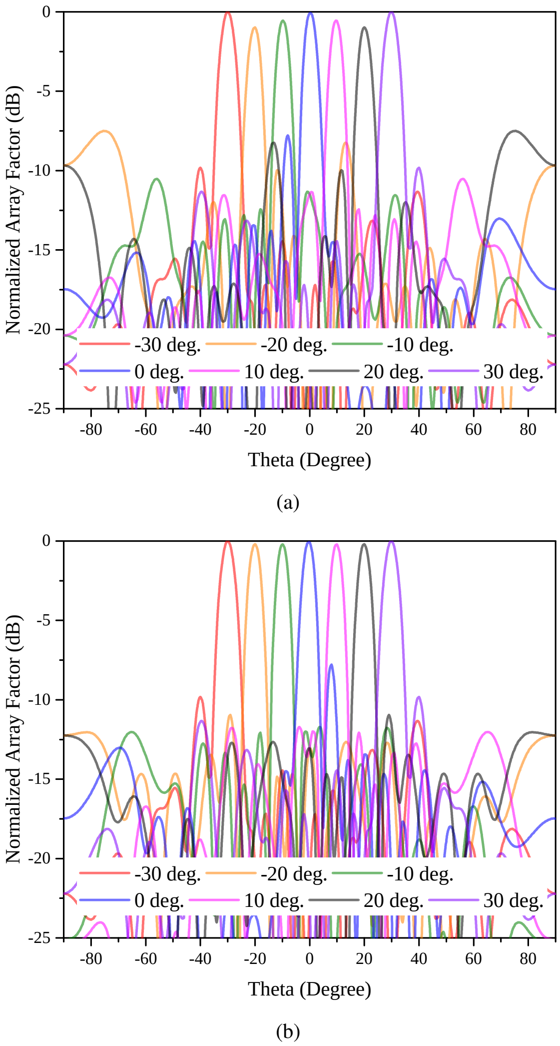

Fig. 3. Numerically calculated patterns for a pseudorandom uniformly distributed prephase: (a) Without considering reference phases; (b) considering reference phases.

1	1	1	1	0	0	1	0	1	0	0	1	1	0	0	1	1	1	0	1
1	0	1	0	0	0	1	0	1	0	0	1	1	0	1	1	0	1	0	1
1	1	1	1	0	1	1	0	1	0	0	1	1	0	1	1	1	1	1	1
1	0	1	0	0	1	1	0	1	1	0	1	1	0	0	0	0	1	0	1
0	0	0	0	0	0	1	0	0	0	0	1	1	0	0	0	1	1	1	1
0	0	1	1	0	0	1	0	1	1	0	1	1	0	1	1	0	0	0	0
1	1	1	1	1	1	1	1	0	1	0	1	1	1	1	1	1	1	1	1
0	0	0	0	0	0	1	1	1	0	0	1	1	0	0	0	0	0	1	1
1	1	1	1	0	1	0	1	0	0	0	1	1	0	0	1	1	1	0	0
0	0	0	1	0	1	1	0	0	1	0	1	1	1	1	0	0	0	0	0
0	0	0	0	0	0	0	0	0	0	0	0	1	0	0	0	0	0	0	0
1	1	1	1	1	1	1	1	1	1	0	0	1	0	0	0	0	1	1	1
1	1	1	1	1	1	1	1	1	1	1	1	1	1	1	1	1	0	0	1
0	0	0	0	0	0	1	0	0	1	0	0	1	0	0	0	1	1	1	0
0	1	1	0	0	1	1	0	0	1	0	0	1	0	1	1	0	0	0	1
1	1	1	0	0	1	1	0	1	0	0	0	1	0	1	0	0	1	1	0
1	0	1	0	1	0	1	0	1	0	0	0	1	1	0	0	1	0	0	1
1	1	1	1	1	0	1	0	1	0	0	1	0	1	0	1	0	0	1	0
0	0	1	0	1	0	1	1	0	0	0	1	0	1	0	1	0	1	0	0
1	1	1	1	1	0	1	1	0	0	0	1	1	0	1	0	1	0	0	0

Fig. 4. Prephase distribution of a planar array, where 0 in the symmetric matrix represents the prephase of 0 and 1 represents the prephase of $\pi/2$.

differential evolution algorithm (DEA), a set of x_k ([8 10 5 10 13 11 2 13 9 12 19 6 2 14 11 10 11 9 12 9]) is obtained for SLLs better than -13 dB in the scanning plane. Here, the DEA is only an optimization tool in this work. Other optimization tools can also be used to find x_k. This result approaches the theoretical SLLs of phase-controlled point source arrays with ideal phase compensation. The worst SLL is improved by nearly 5 dB compared with the random prephase distribution cases.

After optimizing x_k, the numbers of 0 and $\pi/2$ prephases in each column can be obtained. The main issue for the design is arranging the prephases in each column to suppress SLLs and symmetric beams in the whole space (3D patterns). A symmetric matrix is utilized for the design to solve this issue, as shown in Fig. 5. The numbers of 0 and $\pi/2$ prephases are the same for the k-th column and k-th row. Although x_k is optimized for the beam scanning patterns in the xoz plane, the SLL can be suppressed in the whole space because this arrangement can bring a nonperiodic phase quantization error and a noneven function of the array factor. Furthermore, the same scanning range with suppressed SLLs is also achieved in the yoz plane using the same prephase distribution because of the symmetric matrix. Using the 1-bit phase compensation and the symmetric prephase distribution in Fig. 4, the simulated SLLs are lower than -13 dB in the scanning plane and lower than -12 dB in the whole space for a beam scanning range of -30 to 30 degrees (10-degree step).

Finally, note that an arbitrary set of x_k cannot be transformed into a symmetric matrix, and the existence of the symmetric matrix should be considered in the optimization of x_k.

B. 1-Bit State Optimization for Further SLL Suppression

As discussed in Section II, the states of unit cells can be calculated using (4) and (5). The principle is to obtain the maximum energy in the desired direction. In this part, we control some of the unit cell states to suppress the SLLs rather than obtain the maximum power. Therefore, the SLLs can be further suppressed at the price of reducing the maximum RCS in the desired direction.

As discussed, a taper amplitude can help improve the SLL performance, and phase control of the unit cells in a planar array realizes equivalent amplitude control for the scanning plane. Therefore, the states of the unit cells in the four corners are optimized for SLL suppression, and the states of the unit cells in the center are calculated using array synthesis ((4) and (5)) for maximum RCS. In Fig. 5, array synthesis is used to calculate the states of the unit cells in the white area, and a genetic algorithm (GA) is used for the other states in the gray area to optimize the SLLs. The GA is only a tool for optimization and is not the only method that can be used.

The final simulated beam scanning patterns for the point source array are presented in Fig. 6. The simulated SLLs in the whole space are better than -14.95 dB for beam scanning after optimization of the states of some of the unit cells.

0	0	0	1	0	1	0	1	0	1	1	0	0	1	1	1	0	1	1	1
0	0	0	0	1	0	0	0	0	0	0	0	0	0	0	0	0	0	1	1
1	1	1	0	0	1	1	0	1	0	0	1	1	0	1	1	0	1	1	1
1	1	1	1	1	1	1	1	1	1	1	1	1	0	1	1	0	1	1	0
1	1	1	0	0	1	0	1	1	1	1	0	0	1	1	1	0	0	1	0
0	0	0	0	0	0	0	0	0	0	0	0	0	0	0	0	0	0	0	0
1	1	1	1	1	1	1	1	0	1	0	1	1	1	1	1	1	1	1	1
1	1	1	1	1	1	1	1	1	1	1	1	1	1	1	1	1	1	1	1
0	0	0	0	1	0	1	0	1	1	1	0	0	1	1	0	0	0	1	1
0	0	0	0	0	0	0	0	0	0	0	0	0	0	0	0	0	0	0	0
0	0	0	0	0	0	0	0	0	0	0	0	1	0	0	0	0	0	0	0
1	1	1	1	1	1	1	1	1	1	1	1	1	1	1	1	1	1	1	1
0	0	0	0	0	0	0	0	0	0	0	0	0	0	0	0	0	1	1	0
0	0	0	0	0	0	0	0	0	0	0	0	0	0	0	0	0	0	0	0
0	1	1	0	0	1	1	1	1	1	1	1	1	1	1	0	1	0	0	1
1	0	1	1	1	1	1	1	1	1	1	1	1	1	1	0	1	0	0	1
0	1	0	0	0	1	0	1	0	1	1	1	0	0	1	1	0	1	1	0
1	0	0	1	0	0	0	0	0	0	0	0	0	0	0	1	0	0	1	0
0	0	1	0	1	0	1	0	0	0	0	1	0	1	0	0	1	1	0	0
1	1	1	1	1	1	1	0	1	1	1	1	1	1	1	1	0	1	1	0

Fig. 5. Final state distribution for the 30-degree beam direction; 0 represents State 0, and 1 represents State 1.

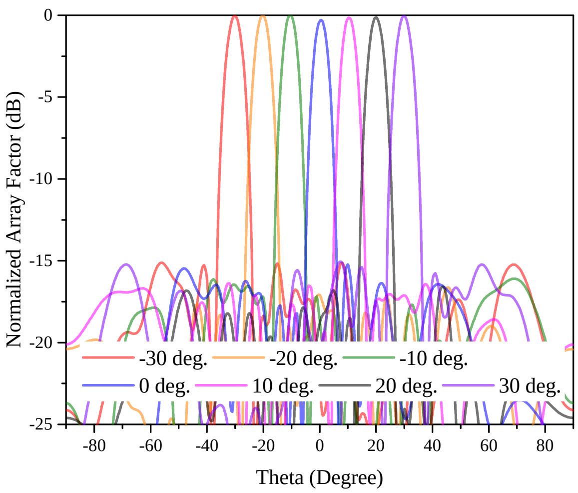

Fig. 6. Scanning patterns from -30 to 30 degrees, using the symmetric matrix for the prephase design and the GA to optimize some of the states.

IV. Design of a 1-Bit Prephase Unit Cell

To verify the proposed method for designing 1-bit phase-only control metasurfaces, a 1-bit prephase unit cell is designed. As shown in Fig. 7, two substrate layers of Taconic TLY with $\varepsilon_{r_1} = 2.2$ are utilized, and the FR-28 laminate with $\varepsilon_{r_2} = 2.8$ is used to bond them together. Vias are used for the metallic cavity design, and the unit cell is in the cavity and etched on the second substrate layer. The structure and working principle of the unit cell are similar to those in [22]. Unit cells without four small stubs are State 0, and those with four small stubs are State 1.

Similar to the physical mechanism for the structure in [22], the current distributions on the unit cells are opposite between State 0 and State 1. Therefore, the metallic cavity reduces the influence between adjacent unit cells, especially for those with opposite states. Furthermore, the via height of the cavity is optimized. The influence between unit cells cannot be suppressed if the height is not sufficient. However, the unit cell performance deteriorates with excess cavity height.

Various patch sizes are utilized for the prephase design, which brings two prephases with a nearly 90 degree phase difference on the same layer. The related parameters are presented in Table I. In other words, the stubs of the unit cells control 1-bit phase compensation, and the unit cells with two different sizes realize a 90-degree prephase difference. In contrast to using the propagation phase difference to design

TABLE I
Parameters of the Proposed Unit Cell for Different Prephases.

Prephase	l (mm)	w (mm)	a (mm)	b (mm)
0-deg.	1.85	0.2	0.8	0
90-deg.	2.75	0.5	0.2	0.925

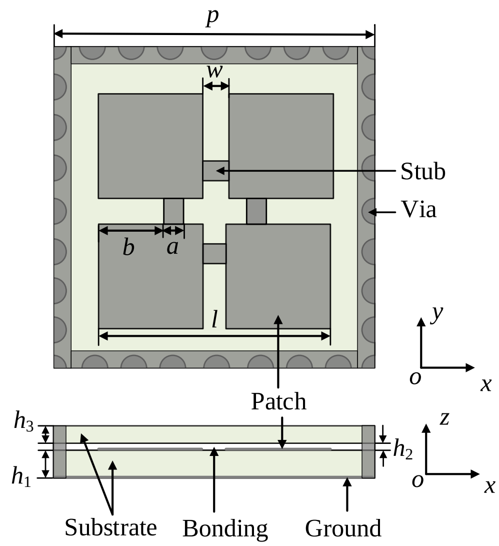

Fig. 7. Configuration of the 1-bit unit cell with p = 4 mm, h_1 = 1.016 mm, h_2 = 0.1 mm and h_3 = 0.254 mm.

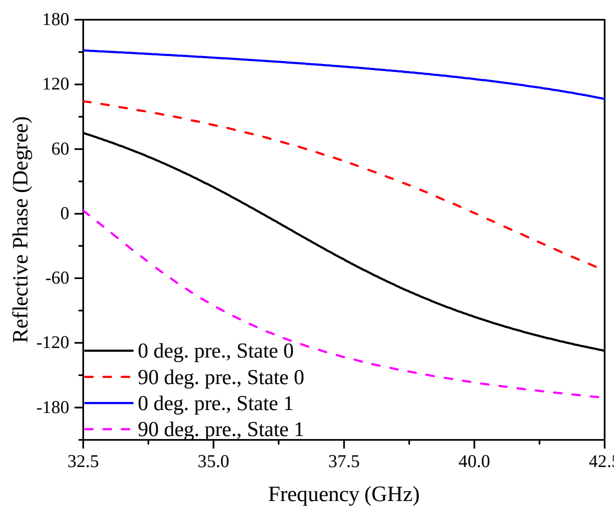

Fig. 8. Simulated reflective phases for the unit cell with different prephases and states.

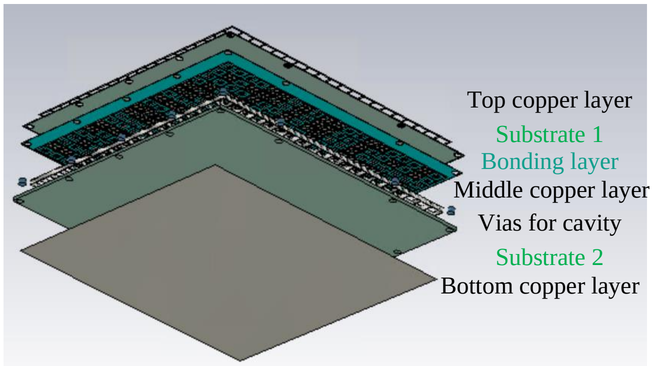

(a)

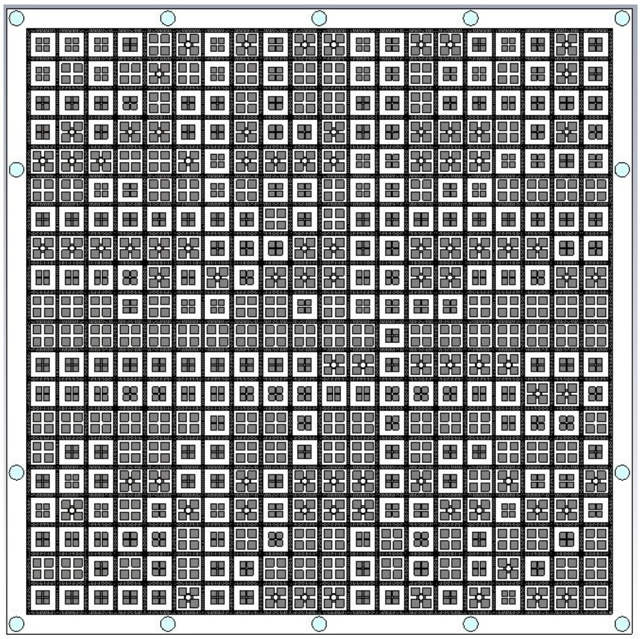

(b)

Fig. 9. Designed 1-bit metasurface with a single-layer prephase structure: (a) 3D model; (b) middle copper layer (30-degree beam direction).

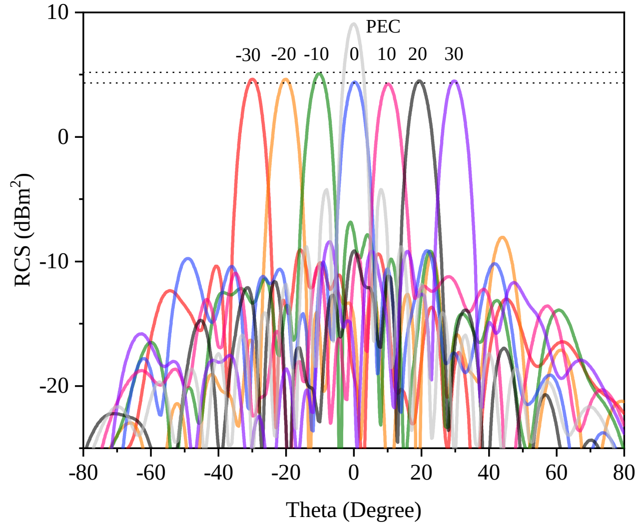

Fig. 10. Scanning patterns from -30 to 30 degrees, simulated RCSs using CST.

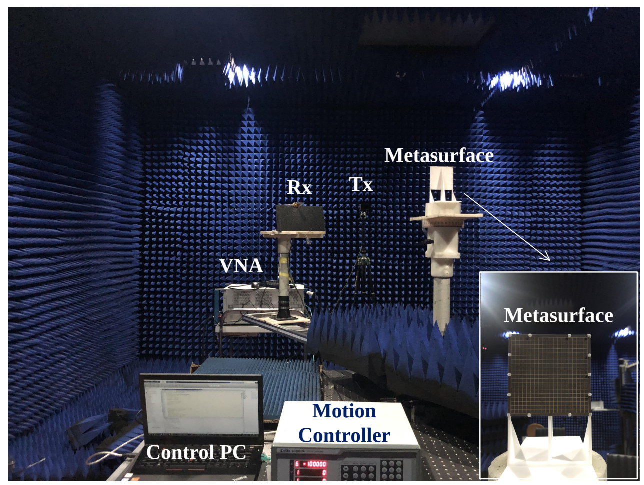

Fig. 11. Measurement setup for the metasurface prototypes.

the prephases of the metasurface [19], this proposed method can enable all unit cells to be on the same layer.

Fig. 8 shows the simulated reflective phases of the 1-bit prephased unit cells. Over the frequency range from 36.5 to 38.5 GHz, the unit cells can achieve an approximately 180 degree phase difference for the same prephase and different states and a nearly 90 degree phase difference for different prephases and the same state.

V. Results and Discussions

A. Simulation Results

A set of 1-bit prephased reflective metasurfaces with suppressed SLLs are designed according to Sections III and IV. The reflective metasurface with a 30-degree beam direction is presented in Fig. 9 as an example, and the unit cells are placed on the middle copper layer. Fig. 9(a) shows a 3D view of the metasurface, and Fig. 9(b) shows the details of the unit cells based on Figs. 4, 5 and 7. The CST simulation results are presented in Fig. 10. The SLLs range from -13.8 to -12.7 dB for beam scanning from -30 to 30 degrees. One main reason for the difference in SLLs with the results in Section IV is that the unit cells are not perfect point sources.

TABLE II
Simulated and Measured Performance of Designed Metasurface at 37.5 GHz.

Sim./Mea.	Level (dB)	Difference with PEC (dB)	SLL (dB)
PEC	9.1/-38.1	0/0	-13.3/-13.1
-30-deg.	4.6/-	-4.5/-	-13.7/-
-20-deg.	4.6/-	-4.5/-	-12.7/-
-10-deg.	5.1/-	-4.0/-	-13.0/-
0-deg.	4.4/-	-4.7/-	-13.8/-
10-deg.	4.2/-43.3	-4.7/-5.2	-13.6/-11.2
20-deg.	4.4/-42.6	-4.7/-5.5	-13.7/-13.6
30-deg.	4.5/-43.7	-4.6/-5.6	-13.1/-12.5

B. Measurement Results and Discussion

Three metasurfaces with 10-, 20-, and 30-degree beam directions are chosen for fabrication and testing from the set

TABLE III
COMPARISONS OF THE PROPOSED PREPHASED 1-BIT METASURFACE AND THOSE IN THE REFERENCES.

Ref.	Element Numuber	Incident Waves	Spacing (λ_0)	Frequency (GHz)	Beam	SLL (dB)
[8]	40×40	Plane Waves	0.5	12.5	10 deg.	-11 (sim.)*
[23]	30×30	Plane Waves	Not Given	10.1	1/2/4 beams	-8 ∼ -3 (mea.)
[19]	20×20	Plane Waves	0.5	39.0	0∼30 deg., step of 15 deg.	-10 ∼ -7 (mea.)
This work	20×20	Plane Waves	0.5	37.5	-30 ∼ 30 deg., step of 10 deg.	-14 ∼ -12 (sim.)
					10 ∼ 30 deg., step of 10 deg.	-14 ∼ -11 (mea.)

∗ The SLL does not include the symmetric beam.

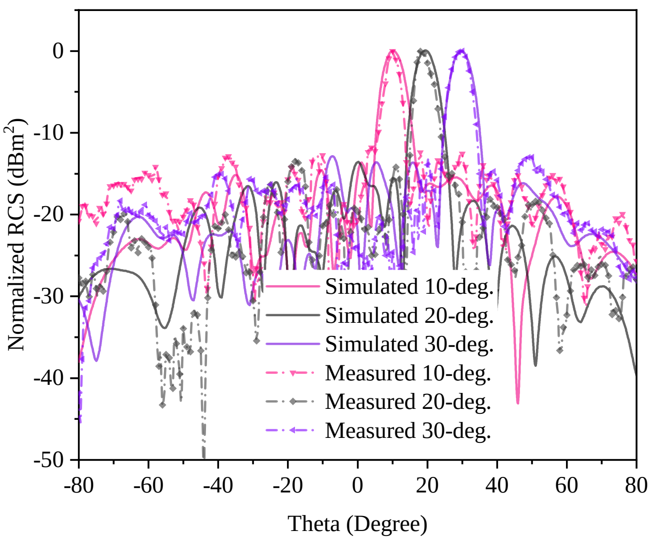

Fig. 12. Simulated and measured patterns for 10-, 20-, and 30-degree metasurfaces under normally incident plane waves at 37.5 GHz.

of designed metasurfaces. The measurement setup is presented in Fig. 11. The horn antenna Tx is fixed and provides approximate plane wave incidence. The horn antenna Rx is aimed at the center of the metasurface and rotates around the metasurface. A vector network analyzer (VNA) is used to record the electrical field level of Rx from -80 to 80 degrees in the horizontal plane, and a control PC is utilized to operate the motion controller and record the data from the VNA.

A copper plate with the same size as the metasurface was also tested as a reference. Table II presents the simulated and measured RCSs and SLLs for different metasurfaces and the copper plate. Fig. 12 shows the simulated and measured patterns at the design frequency of 37.5 GHz. The measured patterns agree with those for the designed directions, and the measured SLLs in the beam scanning plane are suppressed to below -11 dB. This value is slightly higher than that for the simulated SLLs because of fabrication and measurement setup tolerances.

Table III compares the proposed 1-bit reflective metasurface with the reported 1-bit reflective metasurfaces. Under normal plane wave incidence, the SLLs for 1-bit phase-control metasurfaces are usually larger than -10 dB, especially for the worst SLL in the beam scanning range. Additionally, a symmetric beam usually exists in space for single beamforming. Introduction of a fixed random prephase can avoid symmetric beams but cannot suppress SLLs for every beam direction. When the prephase distribution and unit cell states are well optimized and arranged, the SLLs can be effectively suppressed for all designed beam directions. Compared with [19], the proposed SLL suppression method can achieve better SLLs in a larger scanning range. Moreover, the proposed method can significantly reduce the complexity through the prephase number (numbers of 0 and $\pi/2$ prephases in special regions) optimization, rather than prephase distribution optimization. The symmetric matrix also brings a compact prephase design.

VI. CONCLUSION

A prephase synthesis method for SLL suppression of 1-bit phase-only control metasurfaces under plane wave incidence has been proposed. The main idea is to design a fixed prephase distribution for the desired beam scanning range, and the critical issue is to optimize the numbers of 0 and $\pi/2$ prephases in special regions, rather than directly optimizing the prephase distribution. Optimizing the numbers of the two prephases brings equivalent and limited amplitude tailoring for the patterns in the scanning plane, and only N parameters need to be optimized for a metasurface with $N \times N$ unit cells. Then, a symmetric matrix can be used to transform the optimized results (N) into a prephase distribution ($N \times N$). The 1-bit states of unit cells were calculated and optimized for beamforming and SLL suppression. For the 1-bit reflective metasurface design, various sizes were used to realize a single-layer prephase structure. As a demonstration, a set of 1-bit metasurfaces with a fixed prephase distribution were designed. The simulation and measurement results showed that the SLLs can be effectively suppressed by optimizing and arranging prephases to realize equivalent amplitude tailoring. Compared with conventional 1-bit metasurfaces under plane wave incidence, the proposed metasurface can achieve lower SLLs in the designed scanning range.

REFERENCES

[1] T. L. Marzetta, *Fundamentals of massive MIMO*. Cambridge University Press, 2016.

[2] M. Xiao, S. Mumtaz, Y. Huang, L. Dai, Y. Li, M. Matthaiou, G. K. Karagiannidis, E. Björnson, K. Yang, C. I, and A. Ghosh, “Millimeter wave communications for future mobile networks,” *IEEE J. Sel. Areas Commun.*, vol. 35, no. 9, pp. 1909–1935, 2017.

[3] J. Huang, “Reflectarray antenna,” *Hoboken-Piscataway, NJ, USA: Wiley-IEEE Press*, 2007.

[4] C. Huang, A. Zappone, G. C. Alexandropoulos, M. Debbah, and C. Yuen, “Reconfigurable intelligent surfaces for energy efficiency in wireless communication,” *IEEE Trans. Wirel. Commun.*, vol. 18, no. 8, pp. 4157–4170, 2019.

[5] S. V. Hum and J. Perruisseau-Carrier, “Reconfigurable reflectarrays and array lenses for dynamic antenna beam control: A review,” *IEEE Trans. Antennas Propag.*, vol. 62, no. 1, pp. 183–198, 2014.

[6] H. Yang, X. Cao, F. Yang, J. Gao, S. Xu, M. Li, X. Chen, Y. Zhao, Y. Zheng, and S. Li, “A programmable metasurface with dynamic polarization, scattering and focusing control,” *Sci. Rep.*, vol. 6, p. 35692, 2016.

[7] D. R. Smith, V. R. Gowda, O. Yurduseven, S. Larouche, G. Lipworth, Y. Urzhumov, and M. S. Reynolds, “An analysis of beamed wireless power transfer in the fresnel zone using a dynamic, metasurface aperture,” *J. Appl. Phys.*, vol. 121, no. 1, p. 014901, 2017.

[8] H. Yang, F. Yang, S. Xu, M. Li, X. Cao, J. Gao, and Y. Zheng, “A study of phase quantization effects for reconfigurable reflectarray antennas,” *IEEE Antennas Wirel. Propag. Lett.*, vol. 16, pp. 302–305, 2016.

[9] R. J. Mailloux, *Phased array antenna handbook*. Artech house, 2017.

[10] L. Li, F. Qin, L. Wan, Y. Liu, S. Zheng, and H. Zhang, “A wideband 1-bit reflective metasurface based on linear polarizer,” in *2019 Computing, Communications and IoT Applications (ComComAp)*, 2019, pp. 213–215.

[11] J. Han, L. Li, G. Liu, Z. Wu, and Y. Shi, “A wideband 1 bit 12 $\times 12$ reconfigurable beam-scanning reflectarray: Design, fabrication, and measurement,” *IEEE Antennas Wirel. Propag. Lett.*, vol. 18, no. 6, pp. 1268–1272, 2019.

[12] Z. Wang, Y. Ge, J. Pu, X. Chen, G. Li, Y. Wang, K. Liu, H. Zhang, and Z. Chen, “1-bit electronically reconfigurable folded reflectarray antenna based on p-i-n diodes for wide-angle beam-scanning applications,” *IEEE Trans. Antennas Propag.*, vol. 68, no. 9, pp. 6806–6810, 2020.

[13] H. Yang, F. Yang, S. Xu, Y. Mao, M. Li, X. Cao, and J. Gao, “A 1-bit 10×10 reconfigurable reflectarray antenna: Design, optimization, and experiment,” *IEEE Trans. Antennas Propag.*, vol. 64, no. 6, pp. 2246–2254, 2016.

[14] H. Yang, F. Yang, X. Cao, S. Xu, J. Gao, X. Chen, M. Li, and T. Li, “A 1600-element dual-frequency electronically reconfigurable reflectarray at x/ku-band,” *IEEE Trans. Antennas Propag.*, vol. 65, no. 6, pp. 3024–3032, 2017.

[15] P. Mei, S. Zhang, and G. F. Pedersen, “A low-cost, high-efficiency and full-metal reflectarray antenna with mechanically 2-D beam-steerable capabilities for 5G applications,” *IEEE Trans. Antennas Propag.*, vol. 68, no. 10, pp. 6997–7006, 2020.

[16] W. Tang, M. Z. Chen, X. Chen, J. Y. Dai, Y. Han, M. Di Renzo, Y. Zeng, S. Jin, Q. Cheng, and T. J. Cui, “Wireless communications with reconfigurable intelligent surface: Path loss modeling and experimental measurement,” *IEEE Trans. Wirel. Commun.*, vol. 20, no. 1, pp. 421–439, 2020.

[17] D. R. G. Smith, “http://people.ee.duke.edu/$\sim$drsmith/.”

[18] M. Smith and Y. Guo, “A comparison of methods for randomizing phase quantization errors in phased arrays,” *IEEE Trans. Antennas Propag.*, vol. 31, no. 6, pp. 821–828, 1983.

[19] J. Yin, Q. Wu, Q. Lou, H. Wang, Z. N. Chen, and W. Hong, “Single-beam 1-bit reflective metasurface using pre-phased unit cells for normally incident plane waves,” *IEEE Trans. Antennas Propag.*, vol. 68, no. 7, pp. 5496–5504, 2020.

[20] O. Alter, P. O. Brown, and D. Botstein, “Singular value decomposition for genome-wide expression data processing and modeling,” *Proc. Natl. Acad. Sci. U. S. A.*, vol. 97, no. 18, pp. 10 101–10 106, 2000.

[21] D. S. Watkins, *Fundamentals of matrix computations*. John Wiley & Sons, 2004, vol. 64.

[22] J. Yin, Q. Lou, H. Wang, Z. N. Chen, and W. Hong, “Broadband dual-polarized single-layer reflectarray antenna with independently controllable 1-bit dual beams,” *IEEE Trans. Antennas Propag.*, vol. 69, no. 6, pp. 3294–3302, 2021.

[23] T. J. Cui, M. Q. Qi, X. Wan, J. Zhao, and Q. Cheng, “Coding metamaterials, digital metamaterials and programmable metamaterials,” *Light: Sci. Appl.*, vol. 3, no. 10, p. e218, 2014.